Copper diaryl-dithiocarbamate complexes and their application as single source precursors (SSPs) for copper-sulfide nanomaterials

Electronic Supplementary Information (ESI)

Table S1. Crystallographic data and structural refinement details

Complex	**2b**	**2c**	**4**
Empirical formula	$C_{30}H_{28}N_2S_4Cu$	$C_{30}H_{28}CuN_2O_4S_4$	$C_{51}H_{44}CuNP_2S_2$
Formula weight (Å)	608.32	672.32	860.47
Temperature (K)	100(1)	150(2)	100(2)
Crystal system	monoclinic	monoclinic	monoclinic
Space group	$P2_1/c$	$P2_1/n$	$P2_1/c$
Unit cell dimensions			
a (Å)	11.1900(6)	9.7567(2)	18.9452(4)
b (Å)	17.2006(6)	19.5651(2)	12.0938(2)
c (Å)	14.9006(5)	16.5460(2)	19.1076(5)
α(°)	90	90	90
β(°)	97.231(4)	99.443(1)	105.406(3)
γ (°)	90	90	90
Volume (Å^3)	2845.2(2)	3115.68(8)	4220.61(17)
Z	4	4	4
Density (calculated) (g/cm^3)	1.420	1.433	1.354
Absorption coefficient	3.994	3.804	0.730
F(000)	1260	1388	1792
Crystal size (mm)	0.07 × 0.05 × 0.01	0.28 × 0.04 × 0.03	0.38 × 0.025 × 0.02
θ Range for data collection (°)	7.886 to 140.898	7.052 to 145.842	4.04 to 57.436
Index ranges	$-13 \le h \le 12$, $-20 \le k \le 20$, $-17 \le l \le 17$	$-11 \le h \le 11$ $-23 \le k \le 24$ $-20 \le l \le 20$	$-25 \le h \le 25$ $-15 \le k \le 15$ $-25 \le l \le 25$
Reflections collected	21888	51710	51312
Independent reflections	5239	6144	9554
Data / restraints / parameters	5239/0/338	6144/0/482	9554/0/516
Goodness-of-fit on F^2	1.040	1.076	1.026
Final *R* indices [I>2σ(I)]	R_1 = 0.0667, wR_2 = 0.1516	R_1 = 0.0300, wR_2 = 0.0761	R_1 = 0.0834, wR_2 = 0.1866
R indices (all data)	R_1 = 0.0999, wR_2 = 0.1694	R_1 = 0.0338, wR_2 = 0.0786	R_1 = 0.1369, wR_2 = 0.2143
Largest peak and hole(e.Å^{-3})	0.72/-0.59	0.47/-0.37	1.40/-0.78

Table S2. Particle size of copper sulfides as calculated using the Scherrer equation

SSP	**Conditions**	**Phases**	**Crystallite size (nm)**
2b	OLA, 140 °C, HU	CuS	24
2b	OLA, 230 °C, HU	$Cu_{1.84}S$	36
2b	OLA, 230 °C, HI	$Cu_{1.84}S$	35
3	OLA, 230 °C, HU	$Cu_{1.84}S$	60
3	OLA, 230 °C, HI	$Cu_{1.84}S$	50

Particle size of copper sulfides calculated by Scherrer equation, $D = \frac{K\gamma}{\beta cos\theta}$

(Where, D = Crystallite size, Scherrer constant K = 0.9, Wavelength of the X-ray source, γ = 0.15406 nm, β = FWHM, 2θ = peak position)

Table S3. TGA and DSC results for dry [Cu{S_2CN(p-tolyl)$_2$}$_2$] (**2b**) heating rate 10 °C/min.

Solvent	**TGA**		**DSC T °C**	**TGA weight loss (%)**
	Decomposition steps T °C	**Decomposition Temperature (Middle point) T °C**		
Solventless	55.6-247.7 249.8-297.4 300.5-594.1	205.2 266.5 351.9	100 270	3.6 56.6 14.8

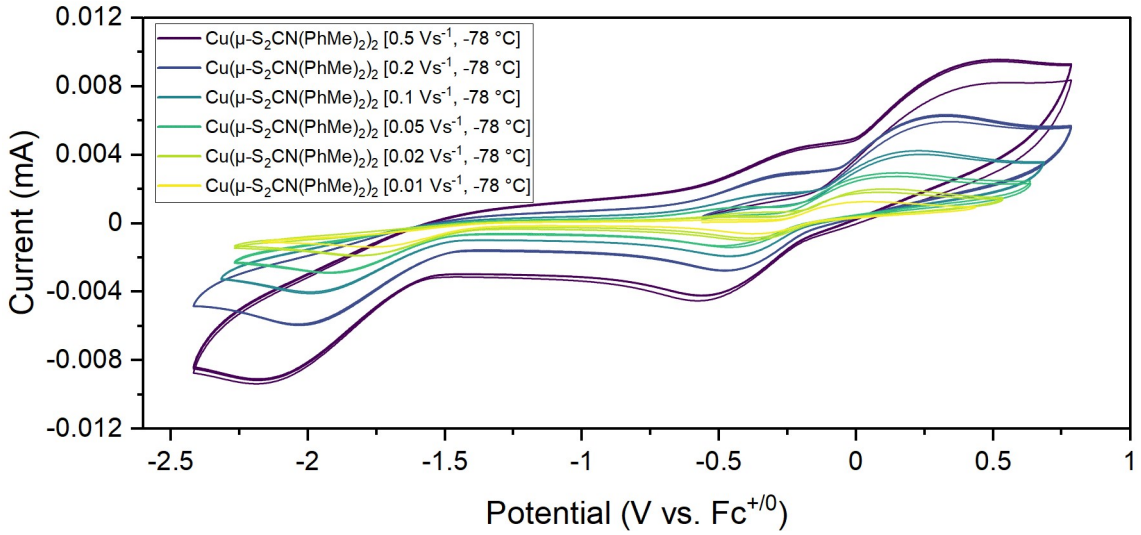

Fig. S1 CVs of **2b** (1 mM) in 0.1 M [Bu_4N][PF_6] in CH_2Cl_2 at -78 °C at a scan rates of 0.02-0.5 Vs^{-1}

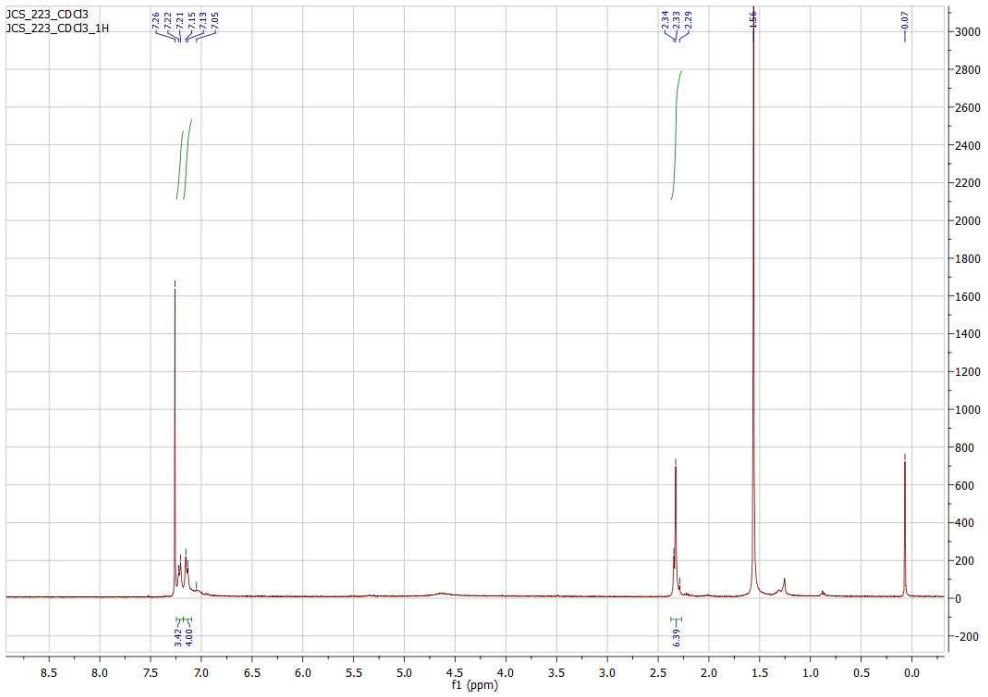

Fig. S2 ^{1}H NMR (in $CDCl_3$) of [Cu{$S_2CN(p\text{-tolyl})_2$}] (**3**)

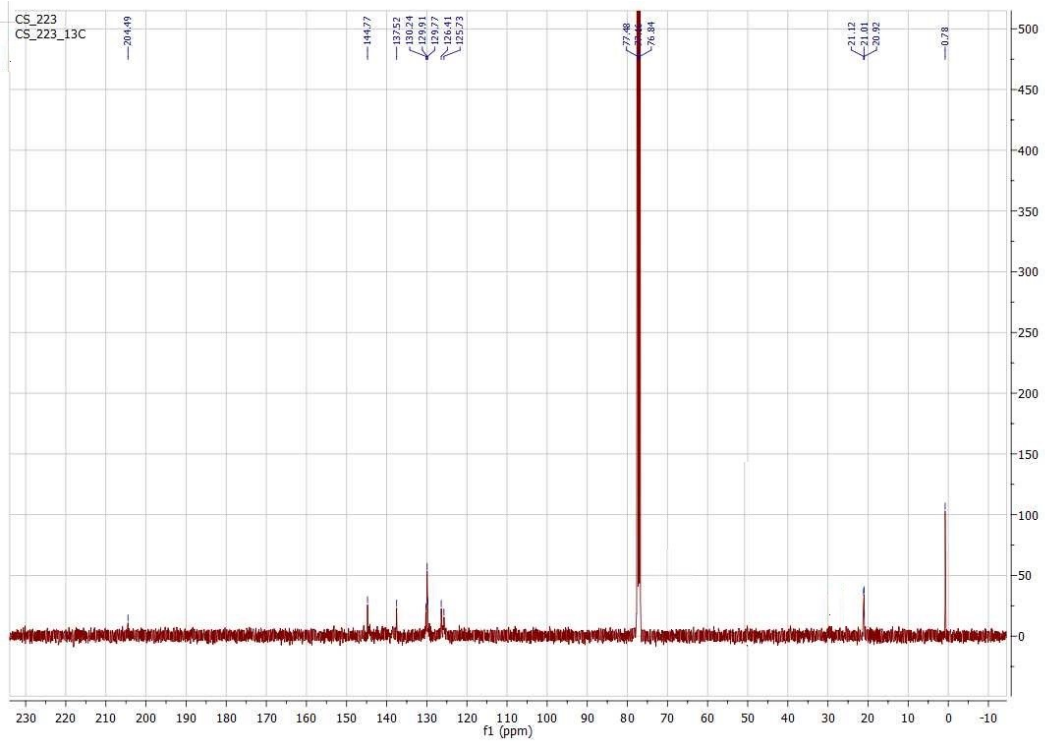

Fig. S3 $^{13}C\{^{1}H\}$ NMR (in $CDCl_3$) of [Cu{$S_2CN(p\text{-tolyl})_2$}] (**3**)

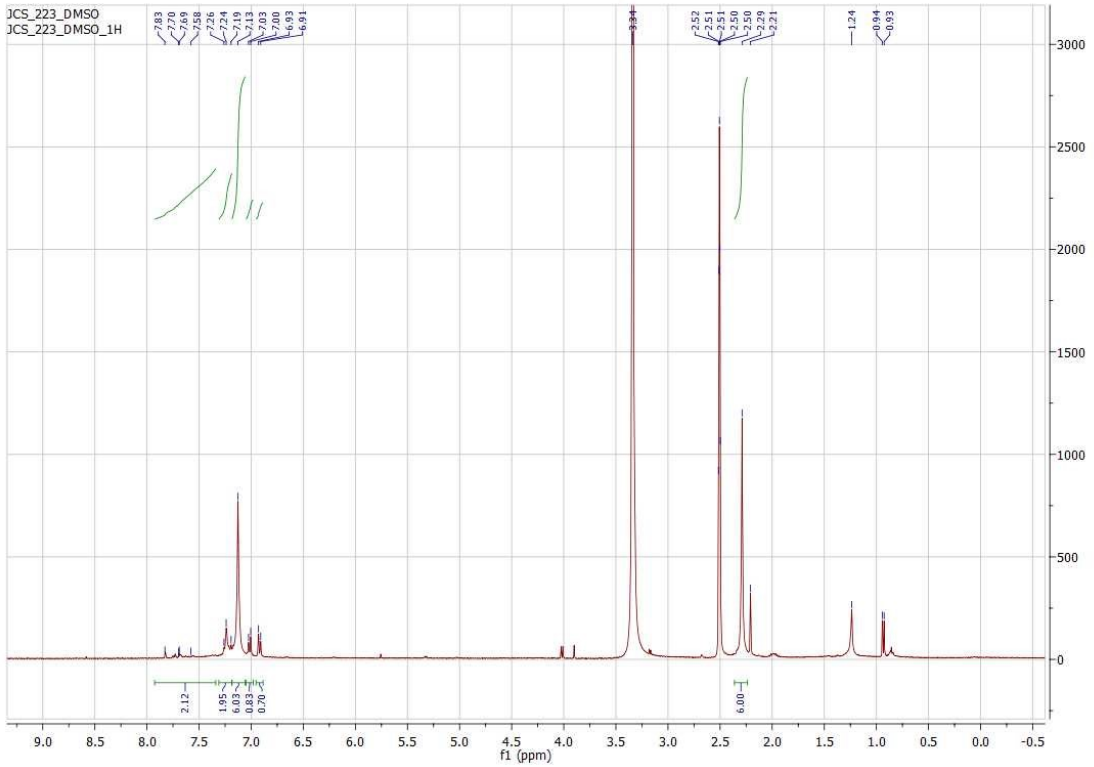

Fig.S4. ^{1}H NMR (in dmso-d^{6}) of [Cu{$S_2CN(p\text{-tolyl})_2$}] (**3**)

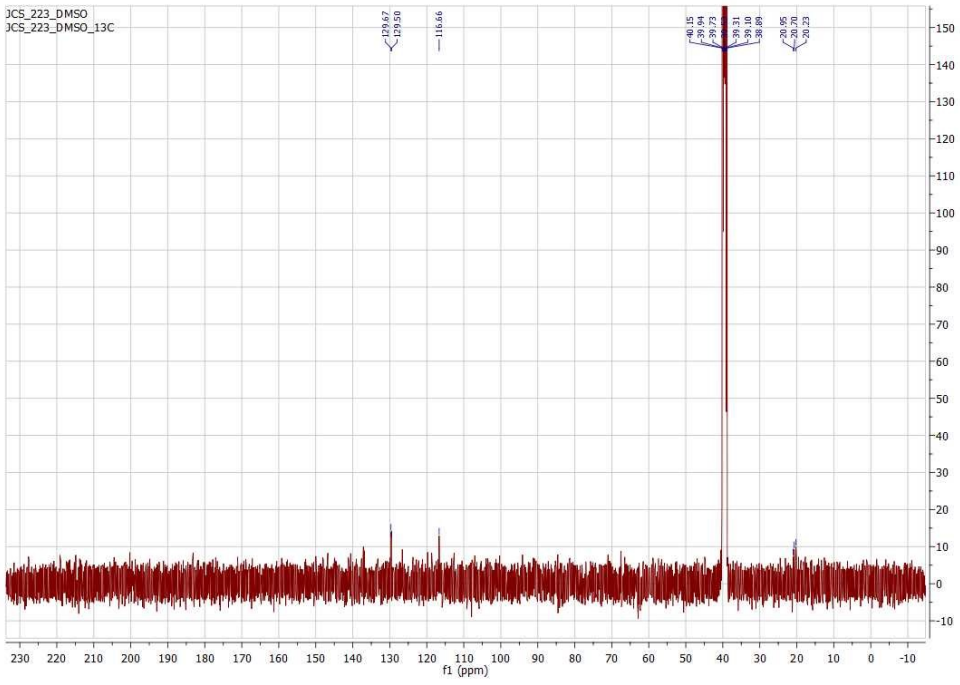

Fig. S5 $^{13}C\{^{1}H\}$ NMR (in dmso-d^{6}) of [Cu{$S_2CN(p\text{-tolyl})_2$}] (**3**)

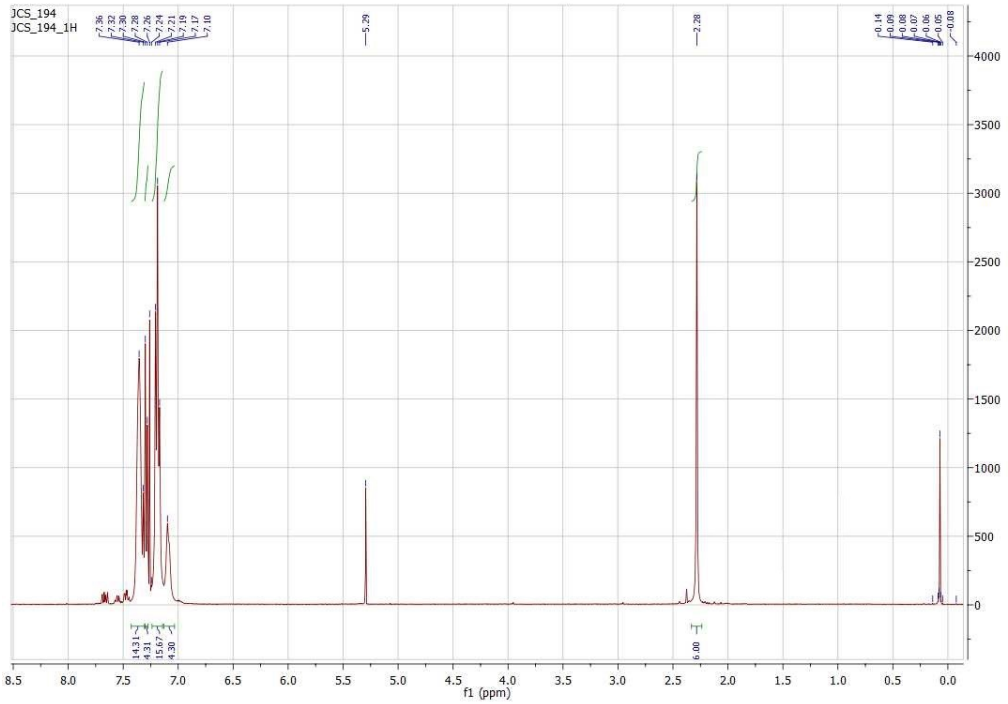

Fig. S6 ^{1}H NMR (in $CDCl_3$) of $[Cu\{S_2CN(p\text{-tolyl})_2\}(PPh_3)_2]$ (**4**)

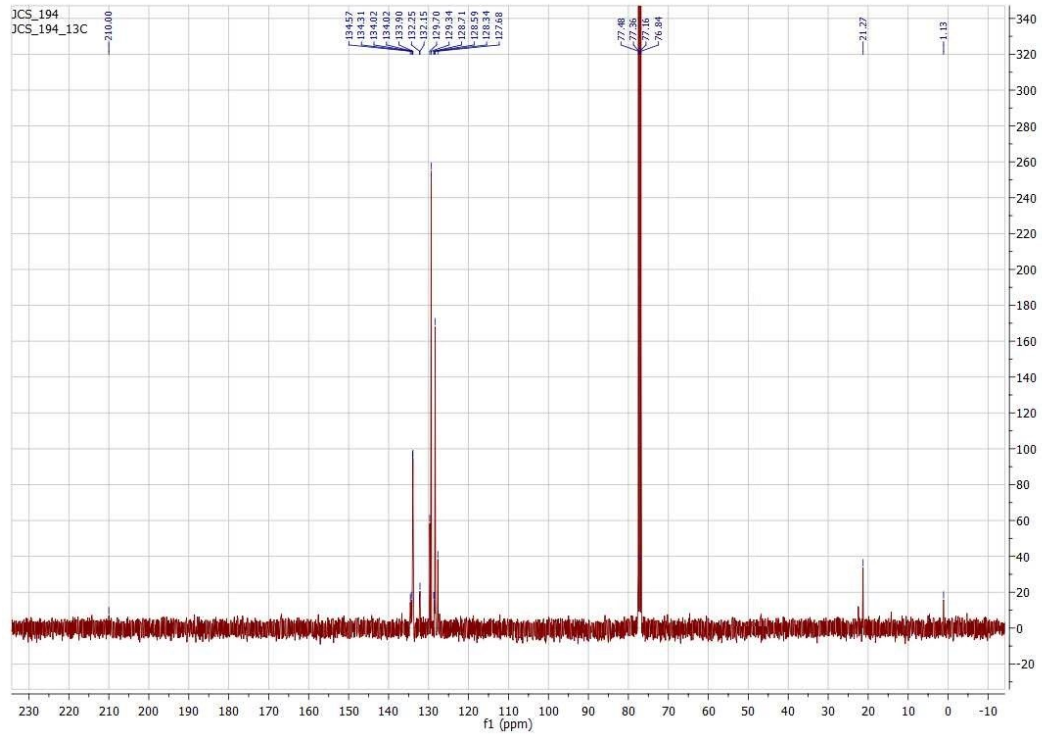

Fig. S7 $^{13}C\{^{1}H\}$ NMR (in $CDCl_3$) of $[Cu\{S_2CN(p\text{-tolyl})_2\}(PPh_3)_2]$ (**4**)

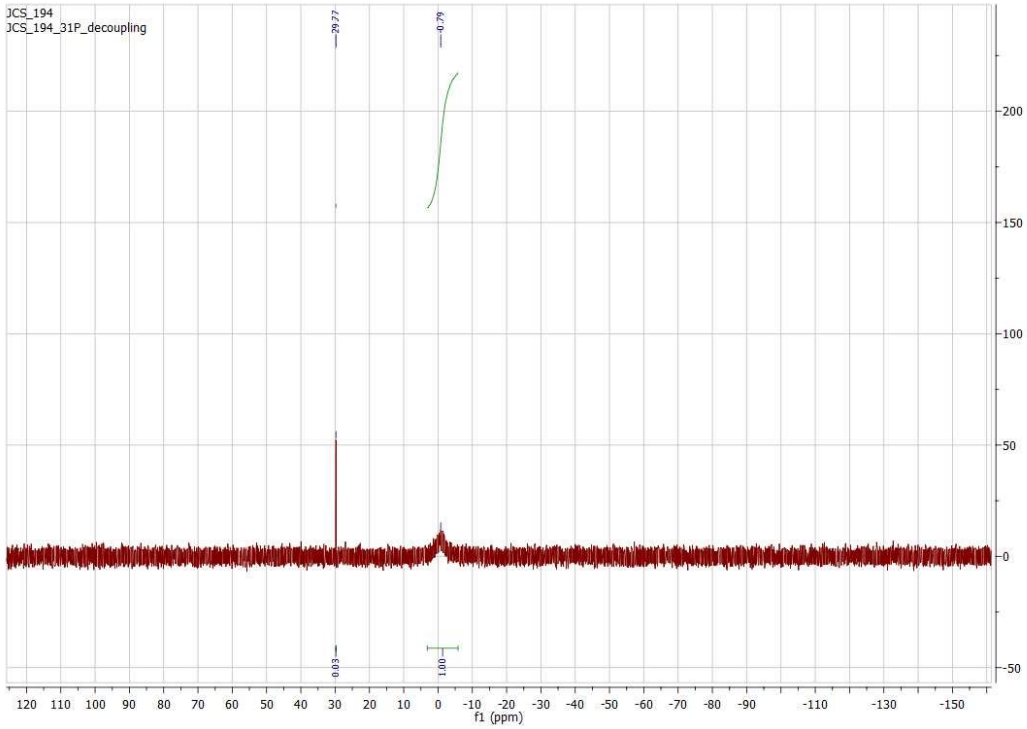

Fig. S8 $^{31}P\{^{1}H\}$ NMR (in $CDCl_3$) of $[Cu\{S_2CN(p\text{-tolyl})_2\}(PPh_3)_2]$ (**4**)

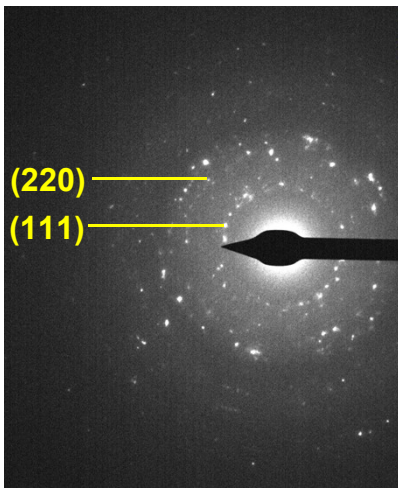

Fig. S9 SAED pattern of $Cu_{1.84}S$ nanoparticles produced from **2b** by HU

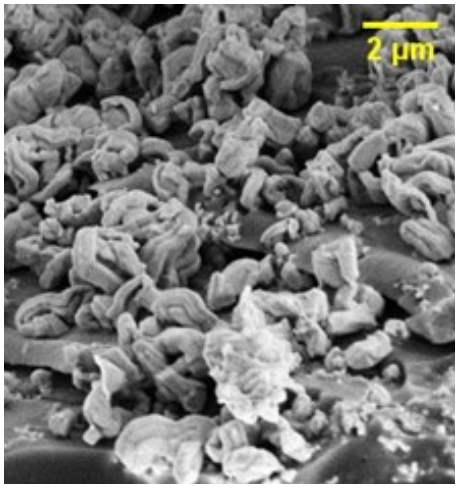

Fig. S10 SEM of nanomaterials formed from dry decomposition of **2b**

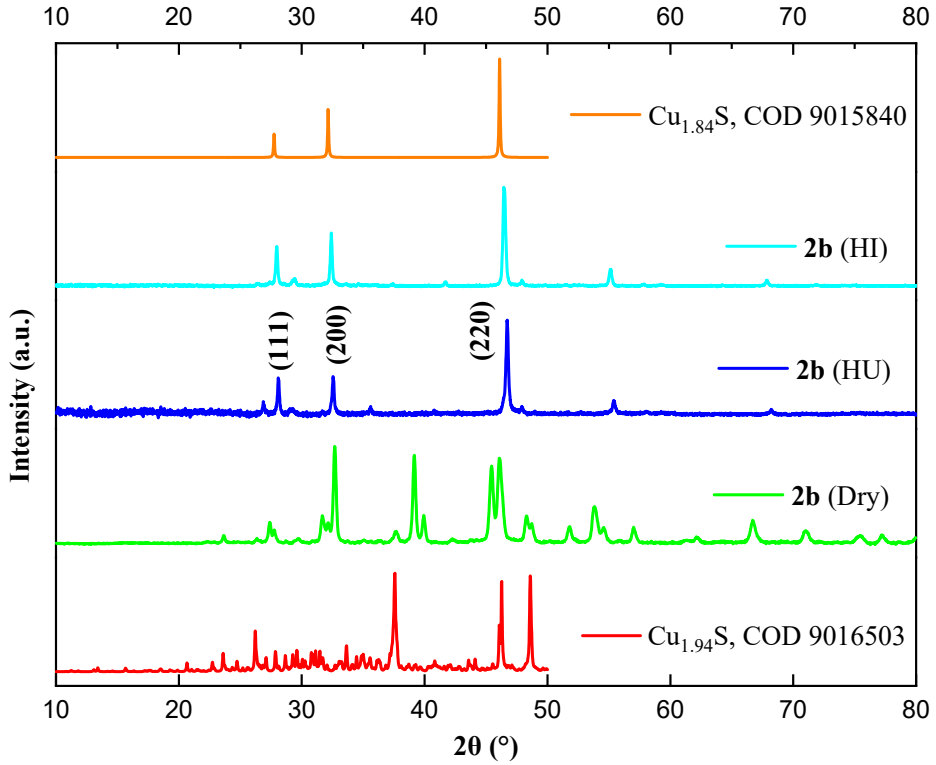

Fig. S11 PXRD pattern of nanomaterials formed from dry decomposition of **2b** compared to those from HU and HI

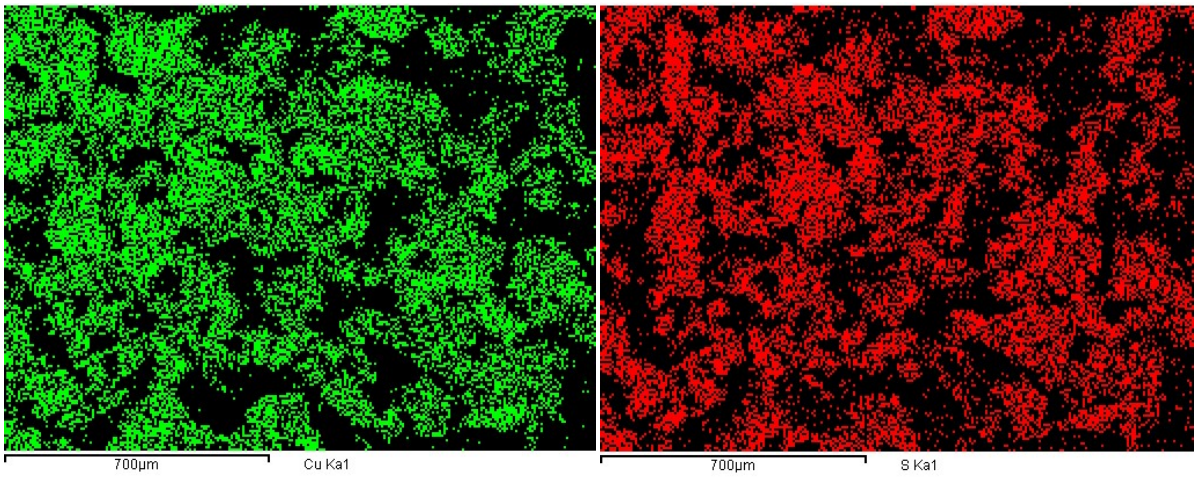

Fig. S12 EDX map of $Cu_{1.94}S$ (worm-like morphology) produced from **2b** by dry decomposition

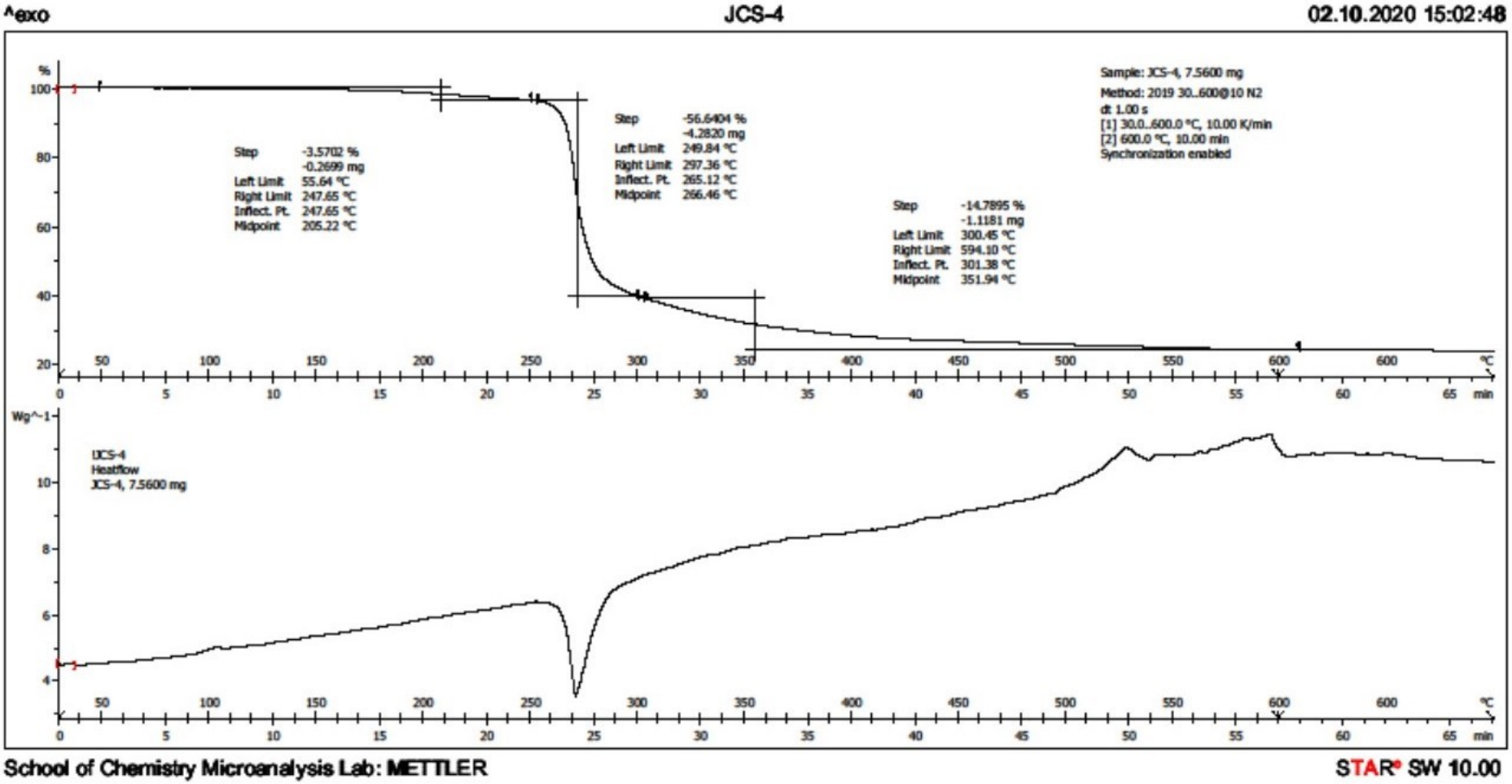

Fig. S13 TGA profile of [Cu{S_2CN(p-tolyl)$_2$}$_2$] (**2b**)